Advances in Textile Engineering

Chapter 1

Biofunctional Textiles

Manuel J Lis[1]*; Meritxell Martí[2]; Luisa Coderch[2]; Cristina Alonso[2]; Fabricio M Bezerra[3]; Ana P Immich[4]; José A Tornero[1]

[1]INTEXTER-UPC, Colon, 15. 08222 Terrassa. Barcelona. Spain.

[2]Institute of Advanced Chemistry of Catalonia (IQAC-CSIC). Jordi Girona 18-26. 08034 Barcelona, Spain

[3]Textile Engineering, Federal University of Technology – Paraná, 635 Marcilio Dias St., Apucarana, 86812-60,Parana, Brazil

[4]Universidade Federal de Santa Catarina, Departamento das Engenharias, Campus Blumenau, SC – Brasil

***Correspondence to: Manuel J Lis,** INTEXTER-UPC, Colon, 15. 08222 Terrassa. Barcelona. Spain*

Email: manuel-jose.lis@upc.edu

Abstract

The aim of the chapter is to state different new possibilities that textile substrates offer for more specialized functions as Biomedical devices, Cosmetics, Skin treatment, and which are the mechanisms involved in such new applications. How to quantify the transport phenomena from the substrate to the skin, or to surrounding different medium, in which they have to be used.

Textiles are covering 80% of the human body and a big percentage of that is in close contact with skin. If the system of vehiculization of the active principles is, carefully, designed, the reservoir effect of the polymeric chains of fibers can play a very interesting role in the delivery of the active principle.

Microencapsulation, lipidic aggregates and nanofibers, have shown very promising experimental results. These results will help to other researchers to develop, more accurate systems, which will valorize textile substrates, fibers and tissues for the use in more sophisticated fields.

1. Introduction

1.1. Textile substrates, as "active systems"

Biofunctional textiles are the textiles with smart and new properties and added value, especially related to comfort or specific functions. Such textiles constitute the basis for the delivery system of cosmetic or pharmaceutical substances when the textile comes into contact with the skin. As most of the human body is covered with some sort of textile, the potential of biofunctional textiles is considerable. Textiles that have functional properties for the skin have been studied and patented in recent years [1,2].

Since time immemorial, textile fabrics have been improved to assist skin function by ensuring homeostasis of the whole body. Practical functions of clothing include providing the human body with protection against the weather –strong sunlight, extreme heat or cold, and rain or snow – and against insects, noxious chemicals and contact with abrasive substances. Clothing offers protection against anything that might injure the naked human body. This is because textiles have always been considered as a "*second skin*" for human beings.

As a result of new technologies, technical bioactive or biofunctional textiles are currently being produced. Such fabrics are able to absorb substances from the skin or release therapeutic or cosmetic compounds to it. The textile industry together with medical knowledge has paved the way for enriching the use of textile fabrics because of their interaction with the skin [3].

Percutaneous absorption is an interdisciplinary subject that is relevant to a number of widely divergent fields. Transdermal devices may be considered as one of the precursors of biofunctional textiles given that they deliver a compound with a therapeutic effect into the body [4, 5].

Bioactive textiles are new, innovative textile products that are pushing back the boundaries of textile applications. They can act as "reservoir systems" and are able to continually release controlled doses of active substances from the textile to the skin. Several active compounds have been applied onto textiles using different vehicles as micro or nanocapsules in order to improve the fixation on the fabric and the progressive and effective release of the active principle into the different skin layers (*stratum corneum*, epidermis or dermis).

1.2. Mechanisms involved and their quantification

1.2.1. Transdermal drug release into the skin

Transdermal drug release is a viable administration route for powerful, low-molecular-weight therapeutic agents that must be precise in its control of drug administration. The system should ensure the required doses and avoid the minimum toxic concentration [6]. This strategy

is especially recommended for many drugs that are difficult to take because they must be delivered slowly over a prolonged period to have a beneficial effect. For instance, the drug release modelling of biodegradable polymeric systems as encapsulation technologies in textiles has not yet progressed appreciably due to its high complexity.

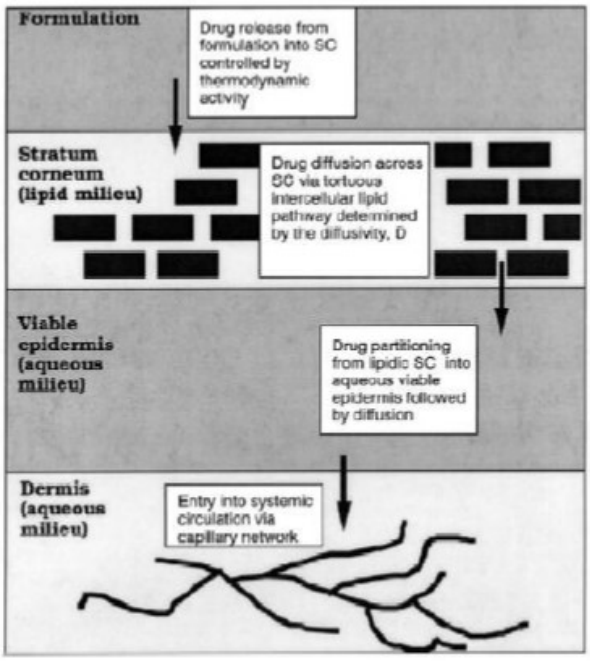

Figure 1: Schematic representation of the transport processes involved in drug release from the formulation up to its uptake through the dermal capillaries [6].

Transdermal administration also can take advantage of chemical and physical strategies that can improve skin permeability and allow for drug penetration [7-14]. Specifically, transdermal drug delivery is a viable administration route for powerful, low-molecular-weight therapeutic agents that either can or cannot withstand the hostile environment of the gastrointestinal tract [6]. Regardless of the necessity for physical-chemical enhancement, for the reliable and effective design of transdermal delivery systems, knowledge of the skin's structure (see **Figure 1**) and its properties is fundamental [9].

Empirical analysis of the permeation of drugs through the skin is based on approaches such as a neural network modelling to predict the permeability of skin [15-22].

Guy and Hadgraft [23] developed a mathematical model for investigating the effect of the variation in thickness during drug release through the skin. Accordingly, the experimental permeation data are fitted by the following equation, which suitable for describing the permeation of a drug through a thin membrane:

$$\frac{M_t}{M_\infty} = \left(1 - \exp\left(-\frac{D_s t}{K L_o L_s}\right)\right) \qquad (1)$$

where M_t is the total amount of drug that passes through the layers of skin, L_s is the thickness of the *stratum corneum* and L_0 the formulation thickness over period t. D_s is the diffusion coefficient of the drug through the different skin layers, and K is a partition coefficient

between the skin layers and the drug formulation (typically K= concentration in skin layer/ concentration in vehicle).

1.2.2. Release mechanisms from vehicles and substrates

The release of an active agent in a non-erodible core-shell system can show different profiles of delivery. In Figure 2, four possible theoretical curves (A, B, C and D) show the global behaviors of the release phenomena in different situations.

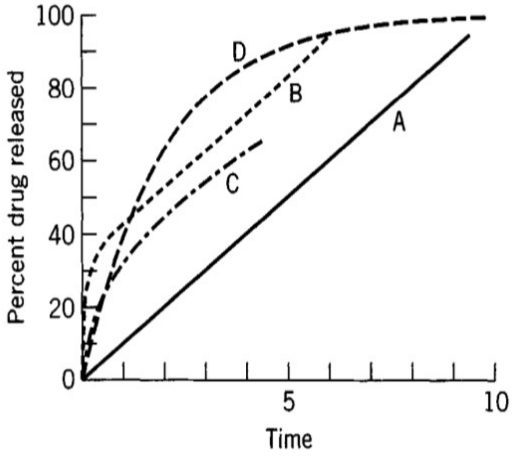

Figure 2: Theoretical release curves expected for different types of non-erodible delivery systems. A, Membrane reservoir-type free of lag time and burst effects; B, same as A, with burst effects; C, matrix or monolithic sphere with square root time-release; D, system with first-order release [24].

Curve A shows a perfect release profile. It shows a system where the rate of delivery is controlled by the diffusion of the active agent molecules through the external membrane. The rate of release depends strongly on the internal-external concentration gradient.

If there exist some molecules that are retained in the shell, then a lag-time on the release will be obtained. Then, there will be two controlling steps and diffusion will undergo a transitional intermediate state. Curve A in Figure 2 displays a system with no lag-time. When the encapsulated material migrates to the external membrane of the microcapsule, there will be a "burst-effect," as shown by line B.

If the microcapsule acts as a microsphere (the entire amount of active agent is distributed in the polymer matrix), the Higuchi equation is useful up to 60% release. In this case, a plot of percent released versus square root of time is linear, as shown by line C. First-order release is represented by curve D. The curve will be linear when the Log of the percentage of core material remaining in the capsule is plotted versus time [25].

The main aim is to apply a mathematic model based on the phenomenology involved, to explain *in vitro* permeation experiments with a biofunctional textile using different molecules, as tracers.

The Korsenmeyer-Peppas, equation (2), can be used to account for the coupled effects of

Fickian diffusion and viscoelastic relaxation in polymer systems by including both processes:

$$\frac{M_t}{M_\infty} = k \cdot t^n \qquad (2)$$

Where M_t is the amount of drug released at time t, M_∞ is the maximal amount of the released drug at infinite time, k is the rate constant of drug release, and n is a diffusional exponent that depends on the system geometry, and the value of n is indicative of the release mechanism of the active agent.

Table 1: Drug delivery models based on the parameter n.

n	Drug Delivery Systems
$n \leq 0.5$	Fickian Diffusion Mechanism
$0.5 < n < 1$	Anomalous Diffusion
$n \geq 1$	Non-Fickian Diffusion Mechanism (zero-order model)

Eq (2) has been used frequently in the literature to describe the relative importance of transport mechanisms as shown in Table 1 [26-32].

Historically, the first mathematical model of drug permeation through the skin was that proposed by Higuchi. Since the establishment of the model, many other authors have conducted excellent research studies on this topic, developing several models based on changes in active principle concentrations

The transport in polymeric organized systems can be described by Fick's second Law, so the diffusion of the active agent can be assumed as a plane surface for short times of liberation, using the Higuchi equation (eq. 4) for to calculate the apparent diffusion coefficient, using the approximation of eq.(3), where D is the apparent diffusion coefficient of drug release, and δ is the width of the planar matrix.

$$\frac{M_t}{M_\infty} = \sqrt{\frac{4 \cdot D \cdot t}{\pi \cdot \delta^2}} \qquad (3)$$

The most widely used model to describe drug release from matrices is derived from Higuchi for a plane geometry, which is applicable for systems of different shapes as well.

$$\frac{M_t}{M_\infty} = K \cdot \sqrt{t} \qquad (4)$$

2. Active Principles used in Micro/Nanoencapsulation for textiles

2.1. Polymers

Encapsulation is one of the techniques used to apply substances to textiles [33, 34]. Biodegradable polymer micro- or nanoparticles are of great interest as drug delivery systems because of their ability to be reabsorbed by the body. Synthetic aliphatic linear polyesters, such as poly-ε-caprolactone (PCL), are often used in biomedical applications [35] because

they are biocompatible, non-toxic and have certain advantages over other polymers such as PLA (poly lactic acid): (a) the polymers are more stable under ambient conditions; (b) they are significantly less expensive and, (c) they are readily available in large quantities [36].

2.2. Ibuprofen

Ibuprofen was used as active principle-tracer. Ibuprofen is an anti-inflammatory steroid. It is used to relieve symptoms of arthritis, primary dysmenorrhoea, fever, and as an analgesic, especially where there is an inflammatory component. Ibuprofen appears to have the lowest incidence of gastrointestinal reactions adverse of all non-selective non-steroidal anti-inflammatory drugs (NSAIDs). However, this only occurs at lower doses of ibuprofen because the usually advisable maximum daily dose is 1,200 mg. Adverse effects include dyspepsia, nausea, ulcers/bleeding gastrointestinal, increased hepatic enzymes, diarrhoea, constipation, epistaxis, headache, dizziness, priapism, rash, salt and fluid retention, and hypertension.

2.3. Caffeine

Caffeine is other active principle used to prepare biofunctional cotton textiles. Caffeine was selected given its use in several specific therapies and its widespread use in cosmetics because of its stimulating activity on fat metabolism (anti-cellulite action) [37-39]. Especial emphasis was placed on the release of this active principle from the formulations and from the cotton fabrics and on its transdermal delivery in order to reach the target compartment of the skin.

2.4. Gallic Acid (GA)

GA was selected and incorporated into polyamide (PA) through microspheres prepared from poly-ε-caprolactone (PCL). Gallic acid (GA) was chosen as the active agent to obtain a biofunctional textile with antioxidant properties. Antioxidants are natural agents that are used to prevent the external aggression of oxidative stress in human beings. The route to apply different compounds is clearly through the skin. When topically applied, these exogenous antioxidants have been demonstrated to diminish the effects of free radicals by using defense mechanisms similar or complementary to those of endogenous antioxidants [40-41].

2.5. *In vitro* drug release experimental results

After GA encapsulation and application onto cotton (CO) and polyamide (PA) fabrics, the results obtained are shown in **Figure 3.**

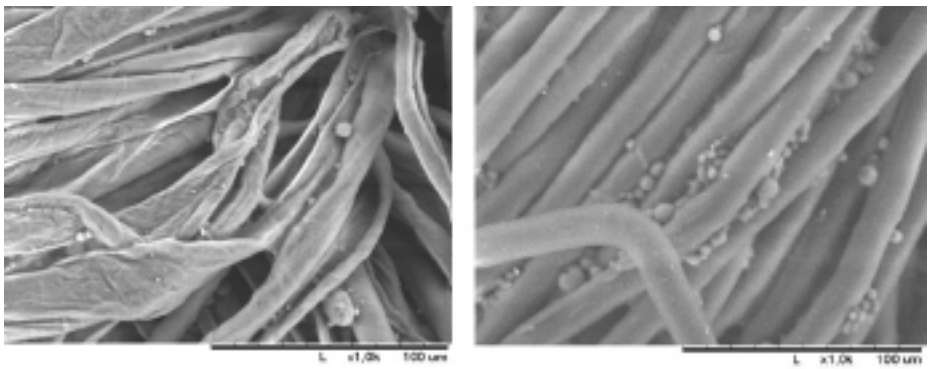

Figure 3: SEM micrographs of PCL-Microspheres with GA. A) Cotton fabric (x1000). B) Polyamide fabric (x1000)

CO fibers allow the microspheres to be placed in corners and spaces which create a proper fiber structure and PA accepts the microspheres between fibers. Visually, PA retains more microspheres than CO. This is in accordance with the higher amount of dry product present in the PA fabric.

To perform the analysis of the mechanism of the drug delivery system, the treated fabric samples were submerged into a semi-infinite bath of physiological saline, and every x minutes, a bath aliquote was picked up and analysed by HPLC.

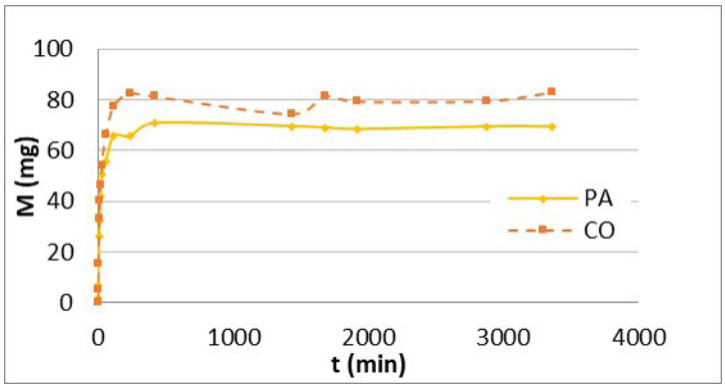

Figure 4: Kinetic release of GA (M) applied on textile fabrics in a bath of serum at 37°C.

In **Figure 4**, it can be seen that PA releases GA more quickly than CO, and PA reaches equilibrium before CO.

Using Eq. (2) on the values of the first steps (**Figure 4**), the exponent n is obtained, which is indicative of the drug delivery mechanism (**Table 2**).

Table 2: n values obtained from fitting drug release experimental data by equation 2.

	n	Drug delivery system
CO fabric	0.46	Fickian diffusion
PA fabric	0.63	Anomalous diffusion

3. Lípids as Vehicles for Skin Treatment

Liposomes are vesicles made up of lipids that can encapsulate different compounds for application onto textiles. Liposomes have been used as models for complex biological membranes in biophysical and medical research owing to their lipid bilayer structural

similarity. Moreover, they have been the subject of numerous studies given their importance as microencapsulation devices for drug delivery and their applications in cosmetics [41-45]. In recent years, liposomes have been used in the textile industry as dyeing auxiliaries, mainly for wool dyeing [46,47] or as a dispersing auxiliary for disperse dyes [48,49].

Wool is a keratinized tissue whose internal lipids have been extracted and analyzed. These lipids are rich in cholesterol, free fatty acids, cholesterol sulphate and ceramides and they resemble those found in membranes of other keratinized tissues such as human hair or *stratum corneum* from skin, because of their capacity to form stable bilayer structures. Accordingly, IWL could be regarded as a new and natural form to encapsulate different active agents or as active agents for skin care [50, 52].

3.1. *In vitro* percutaneous absorption experiments (Franz diffusion cells) and cutaneous effectivity

For these studies, pig skin was used with a thickness of approximately 500 ± 50 μm. Skin discs with a 2.5cm inner diameter were prepared and fitted into static Franz-type diffusion cells.

A control skin disc (without product application on the skin surface) was used to rule out possible interferences in the analysis by HPLC-UV. According to the OECD methodology [5], the skin penetration studies were performed for 24 h of close contact between the textile and the skin. To increase the contact pressure between the textile fabric and skin, permeation experiments were also carried out by placing a steel cylinder on the textile-skin substrate at a constant pressure in accordance with standard conditions (125 g/cm^2) (ISO 105-E04, 1996) (see **Figure 5**).

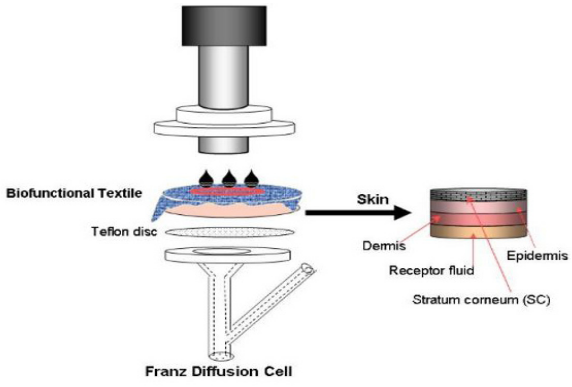

Figure 5: Diagram of *in vitro* percutaneous absorption experiments.

After the exposure time, the receptor fluid was collected, the fabrics were removed from the skin surface and collected together with the top of the cell. The *stratum corneum* of the skin was removed using adhesive. The epidermis was separated from the dermis after heating the skin [53].

The efficacy of the biofunctional textiles in close contact with skin was studied by

measuring changes in transepidermal water loss (TEWL) as an index of skin barrier repair, whereas the water-holding capacity was measured as changes in skin capacitance [54].

Skin tape stripping is an *in vivo* methodology used to demonstrate the penetration of the principle into the outermost layers of volunteer forearm skin [55, 56]. This is a minimally invasive technique to sequentially remove SC by the repeated application of appropriate adhesive tapes [57].

Using these methodologies, it was concluded that liposomes, especially those prepared with IWL, were suitable vehicles for applying a given active principle onto textiles.

3.2. Gallic Acid (GA) encapsulated in lipid structures

GA was encapsulated into liposomes and applied to different fabrics, cotton, polyamide, polyester, acrylic and wool, using bath exhaustion and the pad-dry processes. GA absorption-desorption behavior of the different textiles was compared using the two methodologies (by weight difference and by extraction and detection).

Also, GA was encapsulated in liposomes and in mixed micelles for application to cotton and polyamide. GA absorption-desorption behavior of the textiles was also determined using the two impregnation methods.

3.2.1. Liposome/Mixed Micelle Preparation for Gallic Acid

Liposomes of 4% of Emulmetik 900 (PC) and 2% GA were prepared using the film hydration method reported elsewhere [58]. Mixed micelles (30 wt% of surfactant, 4 wt% of PC and 2 wt% GA) were prepared solubilizing all compounds in distilled water; solubilisation was performed by gently shaking until clear solutions were obtained.

Particle sizes of liposomes and mixed micelles were measured by using Dynamic Light Scattering (DLS), to determine size distribution, polydispersity index and zeta potential of the two lipidic structures.

To quantify the GA entrapped in the vesicles, liposome formulation was precipitated and separated from the supernatant by centrifugation. The efficacy entrapment percentage of GA in liposomes was determined with the amount of the active principle present in the whole liposome solution as well as in the supernatant, using a GA calibration curve.

3.2.2. Textile application and absorption/desorption process.

The application of liposomes or the mixed micelles onto the fabrics was performed by bath exhaustion and the foulard padding process [59].

Liposomes and mixed micelles were also applied to textiles in triplicate with bath exhaustion, liquor ratio 1/5, at 60ºC for 60 min with manual stirring every 10 minutes. To quantify the amount of liposomes or mixed micelles absorbed into the fabrics, the dry samples were weighted before and after 24h application under standard ambient conditions (20±2ºC and 65±5% relative humidity).

Treated fabrics were washed in three different water baths at room temperature. In all cases, the dry samples were weighted before and after 24h of the washing process under standard ambient conditions. The first washing step was performed with deionised water (1/5 liquor ratio) for 5 min with magnetic stirring. A second wash was carried out with deionised water (1/10 liquor ratio) for 5 min with magnetic stirring, and the third wash, with deionised water (1/25 liquor ratio) for 5 min with magnetic stirring. Particle size and zeta potential were measured in the baths after the exhaustion treatment and in the baths after the first and third washings as described for the initial formulations.

The higher substantivity of the phospholipid liposomes for some fibers like PAC, PA and WO was clearly demonstrated by an absorption level higher than 15% for all these fibers. Desorption with water was also evaluated for all the treated fabrics. Results of remaining liposome in percentage are also described in **Table 3**.

Table 3: Percentage of liposome absorbed and desorbed on the different fabrics, CO, PA, PES, PAC and WO using the bath exhaustion methodology. (% owf: percentage over weight of fiber)

	Ini. weightg	Fin. weight % owf	Weight 1st washing % owf	Weight total washing % owf
CO	2.00±0.01	10.99±0.39	7.32±2.43	5.58±0.39
PA	2.05±0.04	16.34±1.23	12.73±1.94	7.31±0.64
PES	2.07±0.01	14.05±1.15	9.64±1.53	2.05±0.50
PAC	1.98±0.06	17.44±1.09	13.20±0.93	4.25±0.33
WO	2.04±0.04	17.15±0.90	12.95±1.05	6.17±0.51

As in the case of the padding process, the highest desorption was obtained for the most synthetic PAC and PES fabrics, followed by CO and WO. The highest retained amount of liposomes was obtained for the PA fabric.

Both liposomes and the textile fibers are usually electrically charged. They are surrounded by a cloud of ions which carry an equal and opposite charge. The zeta potential is the voltage difference between the droplet surface and the liquid beyond the charge cloud. Initial GA liposome formulation applied to textiles has an acidic pH of 3.3 with a zeta potential of -4mV. However, in the washing baths the pH rises to around 5.0 and the zeta potential to around -50mV. The increase in the water layers around a negative charge due to dilution renders the zeta potential more negative. Moreover, the nature of the chemical dissociable groups in the textile fiber surface induces a negative zeta potential of the fibers, see Table 4 [60,61].

Table 4: Z-potentials of textile fibers in aqueous neutral media (83).

	CO	PA	PES	PAC	WO
Pot Z. (mV)	-33	-42	-74	-47	-45

CO is the most hydrophilic fiber, its higher swelling capacity yielding to smaller zeta potential values than the hydrophobic fibers. PAC and, especially PES fibers contain sulfonic and carboxylic groups, respectively, contributing to the most negative zeta potential. Because WO has carboxylic and amino groups near the surface, negative or positive zeta potentials are found when the pH is over or under its isoelectric point 3.5. PA has a moderate hydrophilicity, inferior to cotton but superior to PES and PAC. Moreover, its weakly basic amino groups and weakly acidic carboxylic acid groups give rise to the ionic properties similar to WO.

In the absorption process at pH 3.3, most of the fabrics have a neutral or cationic character with the result that absorption is similar. In the washing baths at pH ≈ 5 and more negative zeta potential, textiles also have higher negative values. The desorption of the PES and PAC (the fibers with the most negative zeta potential) is therefore about 85% and 75%, respectively. By contrast, desorption of WO, PA and CO (the fibers with the least negative zeta potential) is about 65%, 55% and 50%, respectively. The highest fixation properties demonstrated by the lowest desorption of PA and CO, together with the highest comfort properties of these fibers when in contact with the skin, endorse their application as cosmetic biofunctional textiles.

In mixed micelles, the two constituent phospholipids and the surfactant agent are structured together in small micelles, giving rise to a transparent solution. However, dilution of mixed micelles promotes the separation of the surfactant and the phospholipids with formation of liposomes. This results in a large increase in size, giving rise to a turbid solution [62]. The absorption of micelles by textiles could be maintained after a washing process because of an expected increase in size of the vehicles inside the fiber. This could enhance the fixation in textiles with less desorption as occurs in the skin [63,64].

This was expected, owing to liposome formation with dilution. Besides, zeta potential is always negative with small values for the two concentrated formulations around -4mV (Table 5). They increase with dilution in absolute value to -20mV for the mixed micelles and to -50mV for liposomes. These increases in negatively charged are due to the repulsion charges in the dilutions, which increase the colloid stability.

Table 5: Mean size, polydispersity index and Z potential of initial liposome and mixed micelle formulations and their dilutions.

Formulation	Mean Size (nm)	Polydispers. Index	Z-Potential (mV)
Liposome 4% PC	717.40±56.25	0.74±0,03	-4.3±0.30
Liposome 0.4% PC	407.47±24.07	0.79±0,03	-46.3±1.08
Liposome 0.2% PC	367.80± 8.51	0.84±0,10	-49.2±0.90
Liposome 0.1% PC	395.07± 28.84	0.60±0,14	-57.1±0.20
Mix. Micelle 4% PC	8.05± 0.08	0.13±0.02	-4.07±0.01
Mix. Micelle 0.4% PC	8.23±0.17	0.10±0,01	-8.69±1.28
Mix. Micelle 0.2% PC	10.53±0.06	0.14±0.05	-20.47±1.17
Mix. Micelle 0.1% PC	55.35±0.08	0.09±0.01	-19.13±0.29

As in the liposome formulation, the application of the active agent vehiculized in mixed micelles (36% of dry product and 2% GA) to the textile substrates, CO and PA was performed by the foulard process in an attempt to achieve a pick-up of approximately 90-100%.

When mixed micelles were applied to the fabrics, there were differences of about 35% between the calculated amount of product impregnated (34-35%) and the product found in the fabric after heating at the Stenter (22-23%). This could mean that the surfactant, which is the main component of the mixed micelles, has higher substantivity for water than for the textiles. CO and PA incorporate almost the same amount of product (about 23%) which is much higher than the amount of product absorbed with liposomes (see **Table 3**). Desorption with water was also evaluated for the two fabrics. Results of remaining mixed micelles in percentage are also described in **Table 6** and are graphically represented in Figure 6. For comparison, the results obtained with liposomes are also shown.

Table 6: Percentage (% owf) of mixed micelles absorbed and desorbed on CO and PA using the foulard process.

	Ini. weight g	Pick-up tot.% lip%	Fin. weight % owf	Weight 1st washing. % owf	Weight total washings. % owf
CO	2.01±0.10	95.28±3.22 34.3	22.23±1.50	7.07±1.0	1.11±0.13
PA	2.06±0.01	97.6 ±0.5 35.1	23.05±0.63	7.44±0.6	0.26±0.17

The same mixed micelles formulation was applied to cotton and PA by bath exhaustion as described in the experimental section. The initial weights with the percentages of dry product calculated by weight difference between dry initial fabric and dry fabric after bath exhaustion are shown in **Table 7**.

Table 7: Percentage of mixed micelles absorbed and desorbed on CO and PA using the bath exhaustion methodology.

	Ini. weight g	Fin. weight %	Weight 1st w. %	Weight total w. %
CO	2.05±0.04	35,43±2.73	12.72±0.44	2.42±0.06
PA	2.08±0.02	40,14±4.23	18.29±1.98	3.91±0.11

When mixed micelles were applied to the fabrics by bath exhaustion, as in the liposome treatments, higher absorption was obtained for the two fabrics with respect to the pad-dry process, with higher substantivity for PA. The higher temperature of bath exhaustion (60ºC) with respect to the foulard process (30ºC) could account for this. Desorption with water was also evaluated for all fabrics. Results of remaining mixed micelles in percentage are also described in **Table 7** and are represented in **Figure 6** including the results obtained with liposomes.

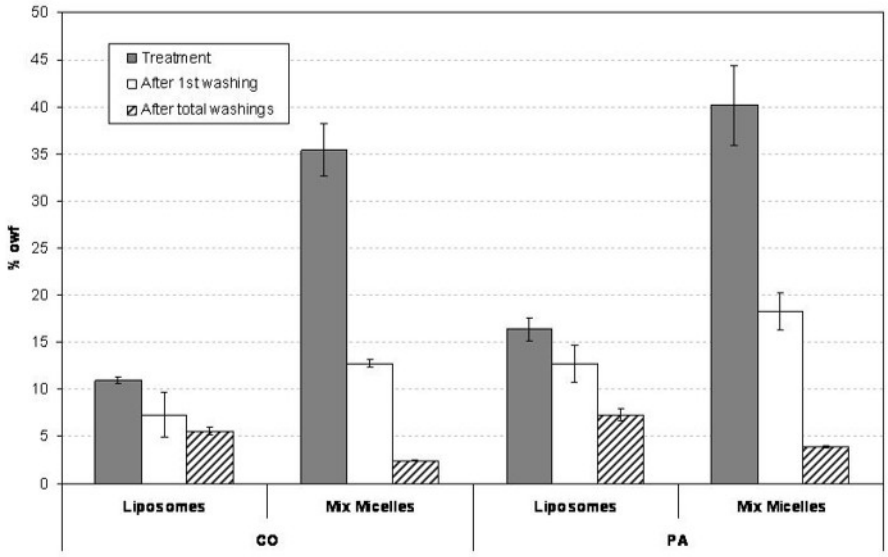

Figure 6: Absorption and desorption of total product (GA in liposome or mixed micelles) applied to cotton and polyamide by bath exhaustion.

As in the case of the foulard process, despite the high absorption, considerably higher desorption was obtained for the mixed micelles treated fabrics with respect to the liposome treated fabrics. Moreover, PA presents higher absorption and less desorption than CO in the case of liposomes and mixed micelles treatments. Interaction of lecithin with CO has been reported to be mainly at the surface through a coating layer, whereas interaction with PA occurs in the interior of the fiber [65].

The higher absorption of mixed micelles in CO and especially in PA could be due to the presence of Oramix in 30%. The increase in particle size with dilution in the washing baths, which could attain 50-100nm, does not prevent desorption. By contrast, a large amount of desorption occurs in mixed micelles treated fabrics. Desorption of PA and CO liposome treated fibers was about 50%, whereas desorption of PA and CO mixed micelles treated fibers attained 90%. The size of the lipid structures of liposomes and mixed micelles was evaluated in the initial and washing baths of the exhaustion treatments (**Table 8**) to determine its possible influence on product desorption.

Table 8: Size (Z-Average) and Polydispersity Index (Pdl) of different baths of CO and PA subjected to bath exhaustion with liposomes and mixed micelles.

Treatment	*Analyzed Bath*	Size (Z-Average) Diameter (nm)	PdI
Cotton/Liposomes	Initial Bath	525.6±26.1	0.68±0.03
	Bath after exhaustion treatment	375.3±64.6	0.51±0.12
	Bath after 1st water washing (10 ml)	474.3±32.2	0.68±0.20
	Bath after 3rd water washing (50 ml)	623.5±18.8	0.52±0.03
Cotton/Mixed Micelles	Initial Bath	6.9± 0.8	0.98±0.04
	Bath after exhaustion treatment	102.2±30.9	0.98±0.03
	Bath after 1st water washing (10 ml)	206.7±76.5	0.34±0.12
	Bath after 3rd water washing (50 ml)	211.0±38.2	0.31±0.02
Polyamide/Liposomes	Initial Bath	525.6±26.0	0.68±0.03
	Bath after exhaustion treatment	460.6±76.4	0.45±0.01
	Bath after 1st water washing (10 ml)	510.0±53.2	0.88±0.21
	Bath after 3rd water washing (50 ml)	660.3±31.9	0.49±0.04
Polyamide/Mixed Micelles	Initial Bath	6.6±0.8	0.97±0.04
	Bath after exhaustion treatment	157.2±81.7	0.62±0.17
	Bath after 1st water washing (10 ml)	257.6±97.9	0.05±0.12
	Bath after 3rd water washing (50 ml)	166.9±89.5	0.34±0.07

The increase in particle size of these structures (see Table 8) did not prevent their exit from the fibers with less desorption as expected. By contrast, desorption was maximum. This could be due to a higher permeability of textiles compared with human skin in which this effect was not observed [63,64].

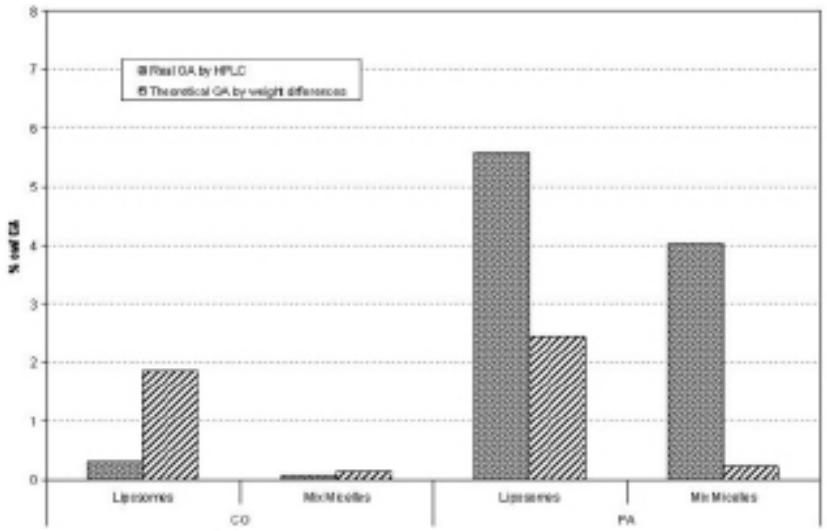

Figure 4: Real and theoretical GA percentages of treated and washed textiles**.**

The lower amount of GA, both real and theoretical, in CO and PA treated with mixed micelles with respect to those treated with liposomes should be noted. The real amount of GA evaluated by HPLC in CO fibers is always lower for the two vehicles than the amount calculated. This is not the case for the PA fiber. These phenomena suggest a low substantivity

for the GA for cotton and a much greater substantivity for PA. It can therefore be concluded that the vehiculization efficiency of liposomes with respect to mixed micelles is always greater for polyamide than for CO. Thus a biofunctional textile with more than 5% of GA is obtained even after three consecutive washings.

4. Electrosupun Nanofibers as Biomedical Devices

4.1. Introduction

Over the past 20 years, the interactions of the fields of polymer and materials science with the pharmaceutical industry have resulted in the development of what are known as drug delivery systems (DDSs), or controlled-release systems [66-69]. Drug delivery systems can be classified according to the mechanism that controls the release of the drug [70], such as diffusion-controlled systems, chemically controlled systems, solvent-activated systems, modulated-release systems and bioerodible-release systems [69-74].

One of the most promising biodegradable polymers for use in bioerodible-release systems is poly(lactic acid) (PLA), Fig 5, because of its mechanical and biological properties.

PLA is a thermoplastic polyester derived from renewable resources, such as corn starch. PLA has a hydrolytic degradation mechanism, and it is capable of degrading into innocuous lactic acid and then into CO_2 and water, which are absorbed by the body. PLA is used in medical implants in the form of screws, pins, rods and as a mesh [75-77]. Depending on the exact type used, PLA degrades in the body within 6 months to 2 years [77]. This gradual degradation is desirable for a support structure because it gradually transfers the load to the body as the organ heals.

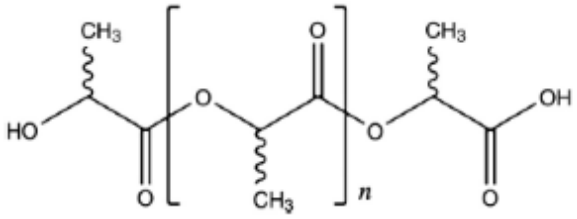

Figure 5: Chemical structure of PLA

Here, the properties of a different drug-delivery system, which consists of different nanofiber membrane configurations, were examined. The membrane configuration was based on sandwiching the drug between two adjacent layers of electrospun PLA membranes to determine the mass transport behavior of the drug through different polymeric membrane configurations.

Similar studies have been conducted by Fied et al. [78] with the purpose of developing ultrafiltration membranes. Tiemessen et al. [79] have also described a so-called occlusion simulation model based on sandwiching the *stratum corneum* between sticky silicone membranes to provide a means for simulating skin penetration under occlusion.

The electrospun PLA membranes were shown to provide a useful mechanical support for the drug. The initial studies on the sandwich model also revealed that this model provides an elegant means to kinetically control the water uptake by the drug. Although the PLA membrane is biodegradable or erodible (i.e., a system that disintegrates over time), this phenomenon can be irrelevant when the entire drug is released before the dissolution of the polymer becomes important. Therefore, the membranes could be considered non-erodible.

Therefore, this new system can be directly used in the prophylactic period of patients who recently underwent an operation, when *in situ* application is required. In some cases, this particular membrane can act not only as a carrier but also as cavity filler with therapeutic agents.

Here, the polymeric solution used to produce nanofibers was obtained by dissolving 10% of the solution weight of poly(lactic acid) in dichloromethane under constant magnetic agitation and at a constant room temperature of 23-25 °C. The magnetic agitation remained constant until the PLA was completely dissolved, which was indicated by the solution becoming translucent and when no solid particles were detected. Complete dissolution was achieved after 1 hour of agitation.

To conduct the experiment, a high voltage power supply, a spinneret (a capillary tube with very small diameter) and a grounded collector plate (a plate usually composed of metal) were required, as seen in **Figure 6.**

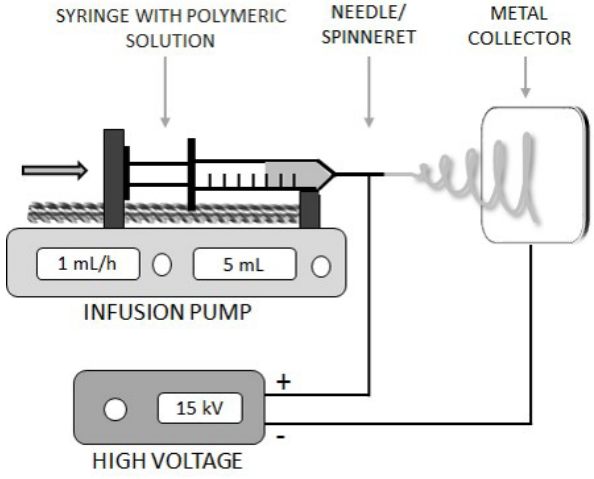

Figure 6: Electrospinning device containing all essential elements: high voltage, spinneret, metal collector

During the electrospinning process, a strong electrostatic field is applied to a polymer solution held in a syringe with a capillary outlet. A pendent-shaped droplet of the polymer solution from the capillary outlet is deformed into a Taylor cone [80] by the electrostatic field. When the voltage surpasses a threshold value, the electric force overcomes the surface tension of the droplet and a charged jet of the solution is ejected from the tip of the Taylor cone. As the jet moves toward a collecting metal screen (counter electrode), the solvent evaporates and a non-woven fabric mat is formed on the screen [81]. The process can be seen in **Figure 7.**

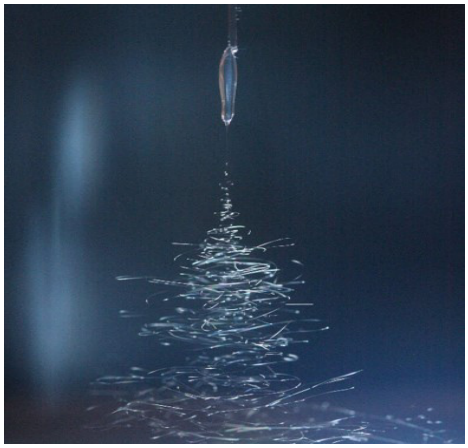

Figure 7: Electrospinning of PLA under optimal conditions

4.2. Experimental results of Nanofibers formation

When applying the former conditions specified, PLA nanofibers are formed, as the following figures show.

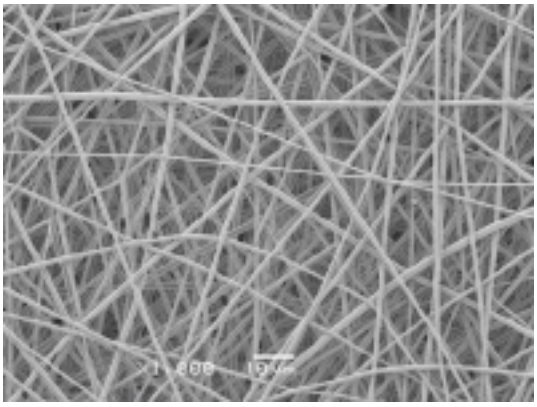

Figure 8: SEM of PLA fibers under optimal high voltage conditions (order of magnitude 1000 x).

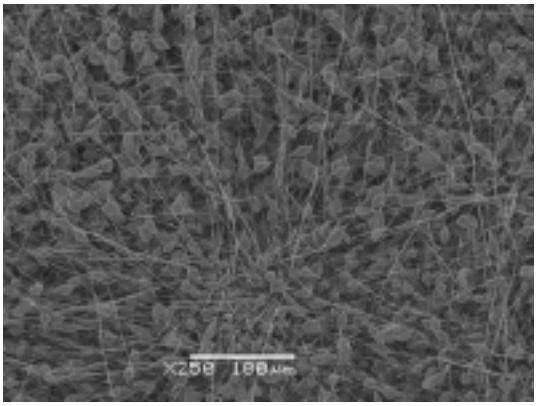

Figure 9: SEM of PLA with bead defects; order of magnitude 250x

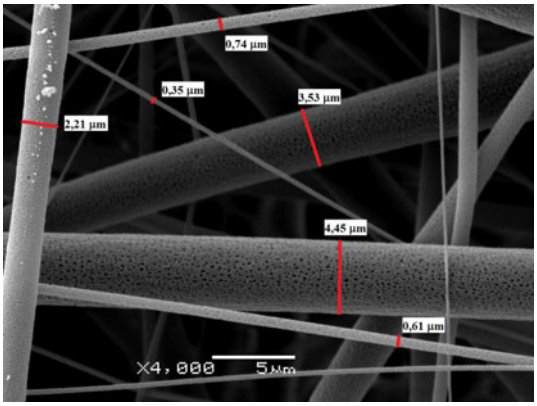

Figure 10: SEM of PLA fibers with increasing flow rate; order of magnitude 4000x.

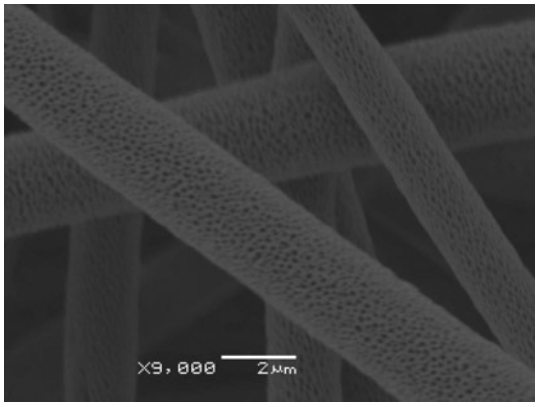

Figure 11: SEM of porous PLA fiber due to high room humidity

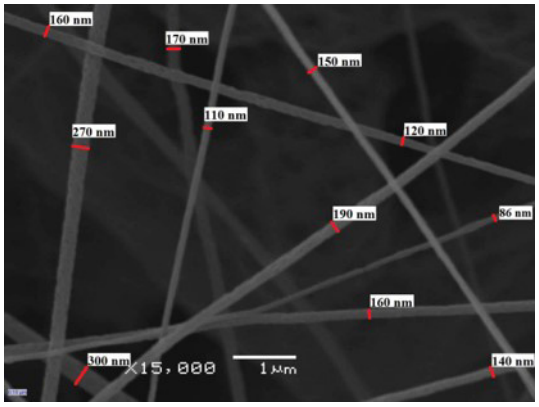

Figure 12: SEM of nanofibers produced by optimized electrospinning process; order of magnitude 15000x.

4.3. Sandwich configuration with *Ibuprofen or Caffeine*

Ibuprofen, or caffeine, was placed between two adjacent layers of the polymeric membranes. When the first layer of the electrospun membrane was dried and solidified, the drug, which was in a dried medium, was evenly dispersed on the membrane surface. The amount of drug was controlled using an analytical balance. After placing the drug on the membrane surface, a second membrane layer was electrospun over the first layer to cover the drug [82].

4.4. Drug-Delivery Mechanisms

The capability of the polymeric membrane to deliver the drug was determined through triplicate measurements of the drug release kinetics into a fluid phase.

The drug release kinetics were determined using batch methods for membranes operating in different conditions, such as membranes obtained after different electrospinning periods (5, 10 and 20 minutes) and sandwich membranes with different drug amounts (5, 10 and 15 mg). For each operating condition, the experiment was repeated 3 times.

To perform the experiment, the sandwich membranes were placed between concentric rings in a metallic tambour system, as shown in Figure 13, to ensure uniform mass transfer along the surface of the membrane from the solid phase to the fluid phase and to so avoid bending stress.

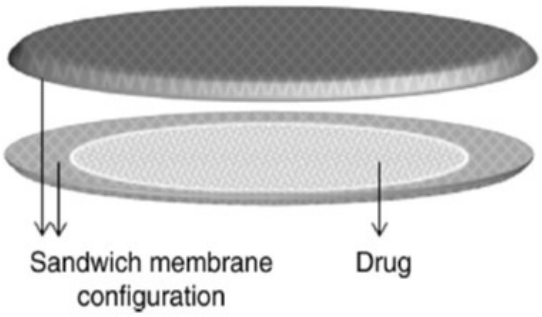

Figure 13: Mass transfer configuration device on the drug-delivery experiment

After adjusting the sandwich membranes in the metallic tambour system, they were placed in a covered container with 100 mL of physiological serum as the fluid phase, with a pH 7.4. The containers prepared for the analyses were maintained in a bath with a constant temperature of 37°C. The samples were taken for analysis at regular time intervals, and the concentrations of drug released into the fluid phase were determined through spectrophotometric techniques in a Shimadzu UV-2401 PC UV-vis spectrophotometer with a wavelength of 263 nm.

4.5. Controlled Drug Release Mathematical Modeling

The results obtained from the kinetics tests were used for the mathematical modeling of the controlled drug release, following the approach explained before in Immich et al.[83] and in 1.2.2.

4.6. Scanning Electron Microscopy (SEM)

The surface morphologies and thicknesses (δ) of the polymeric membranes were examined using a scanning electron microscope (JEOL/JSM-5610). After the samples were dried overnight at room temperature, each specimen was sputtered-coated with gold powder before being examined with the SEM. For the thickness measurement, 3 different regions of the transversal area of the membrane were measured, and the average value of these measurements was used.

The membrane thickness was determined for the PLA membranes obtained after 5, 10 and 20 minutes of electrospinning with different amounts of ibuprofen. The results are presented in **Table 9**.

Table 9: Thickness of PLA membranes for different ibuprofen amounts.

Electrospinning time(min)	*Ibuprofen amount (mg)*	*Membrane thickness (mm)*
5	5	0.0662
5	10	0.0926
5	15	0.1190
10	5	0.0927
10	10	0.1130
10	15	0.1423
20	5	0.1192
20	10	0.1424
20	15	0.1655

The differences in the morphologies of the PLA membranes with different electrospinning time intervals were analyzed and the difference in the amount of fibers in each obtained membrane is noticeable. In the PLA membrane obtained after 5 minutes of electrospinning, it can be seen empty spaces among the fibers. These empty spaces facilitate mass transference of the fluid phase through the membrane, which is readily conducive to drug release. When there is an increase in the amount of fibers and consequently, a reduction in the amount of empty space, the molecular mobility becomes difficult and consequently, it reduces mass transport through the membrane.

The diameter of the fiber in a pure membrane obtained after 20 minutes of electrospinning (without the drug) was also measured using SEM, and the average diameter is approximately 150 nm when disregarding the bead effect.

4.7. Ibuptofen delivery from PLA electrospun membrane

The influence of the membrane thickness on the release kinetics of ibuprofen through PLA membranes was studied at an initial drug amount of 5 mg **(Figure 14)**.

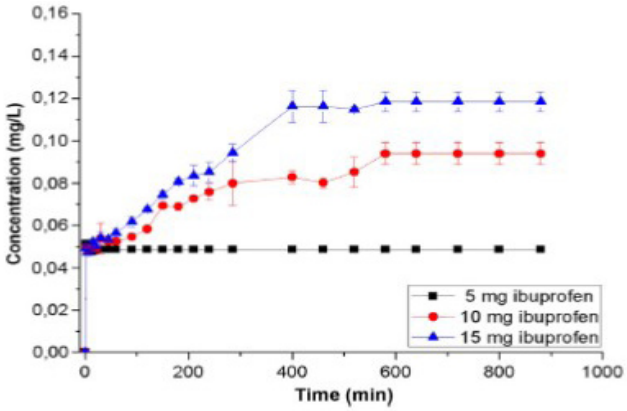

Figure 14: Kinetics of ibuprofen delivery from PLA membranes after 5 minutes electrospinning After the initial burst, the polymer structure swells, stabilizes and traps the drug. The result is a continuous and slower sustained release process.

Although the PLA membrane is biodegradable or erodible, in this study, the phenomenon

was negligible because the entire drug had already been released before the dissolution of the polymer became important. Therefore, the membranes were considered to be non-erodible. Figure 14 presents kinetics behavior with a more intense initial burst, which leads to a release of approximately 0.05 g/L of ibuprofen (100 % of initial drug concentration) during the first stage of the drug delivery.

More controlled release processes are observed in kinetics presented in Figures 15 and 16, with a less intense burst effect and an initial drug release of approximately 0.03 g/L (30% of initial drug concentration) and 0.02 g/L (13% of initial drug concentration), respectively. This decrease in the burst effect intensity is due to an increase in membrane thickness after 10 and 20 minutes of electrospinning, which delayed mass transference through the polymeric membrane to the external fluid phase.

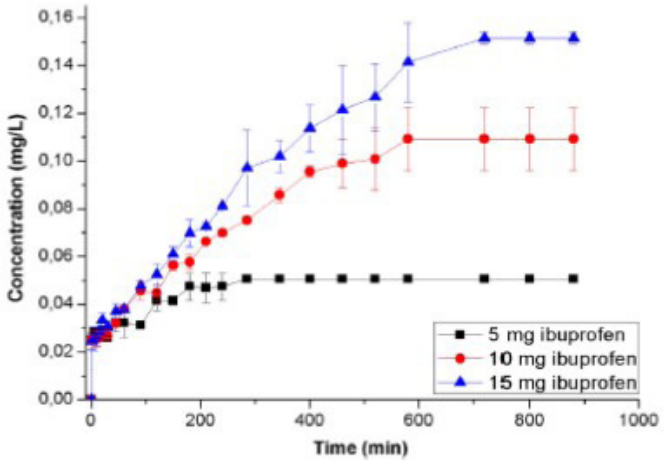

Figure 15: Kinetics of Ibuprofen delivery from PLA membranes after 10 minutes electrospinning

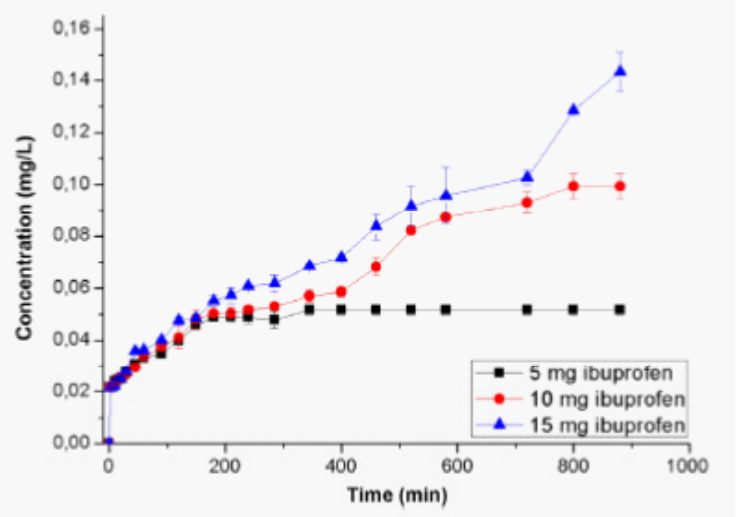

Figure 16: Kinetics of ibuprofen delivery from PLA membranes after 20 minutes electrospinning

In addition to the decrease of the burst effect in drug release for the membrane obtained after 20 minutes of electrospinning, an increase in the pseudo-equilibrium time of total drug release was also observed due to the membrane thickness, which is considerably greater than that of the membrane obtained after 5 minutes of electrospinning. This thicker membrane also restrains and controls drug mobility and transport through the membrane.

The amount of ibuprofen within the membrane is also important when determining the time required for the total release of the drug. When the amount of ibuprofen increases from 5 to 10 mg, the time required for the total release of the drug increases by 72% on average. There is no significant increase in time for the total release of the drug when the amount of ibuprofen increases from 10 to 15 mg. Membranes with 10 and 15 mg of ibuprofen have similar behavior during the releasing process.

Because the kinetics curves for the release of ibuprofen, which are illustrated in Figures 14, 15 and 16, exhibit the typical behavior for reservoir-type membranes, it can be assumed that the drug transport mechanism through these membranes is usually a solution-diffusion mechanism. Though, this is not sufficient to prove the mechanism of drug release. For that reason, the releasing mechanism (n) of ibuprofen was calculated, according to Power Law equation (2) [83].

Table 10: Mechanism of drug release for PLA membranes.

Electrospinning time (min)	*Ibuprofen amount (mg)*	*n (releasing mechanism)*
5	5	0.18
5	10	0.30
5	15	0.31
10	5	0.22
10	10	0.50
10	15	0.50
20	5	0.25
20	10	0.40
20	15	0.40

The releasing mechanism presented in **Table 10**, for polymeric membranes obtained after 5 minutes of electrospinning, do not describe any established mechanism of drug release. It means the mechanism of release is neither a diffusion-controlled drug release ($n=0.5$) nor a swelling-controlled drug release ($n=1$), where the relaxation process of the macromolecules occurring upon water imbibition into the system is the rate controlling step. Here, the reason for the release of ibuprofen must be the large porosity of the thin 5 minute membrane that does not restrict the molecules of ibuprofen from passing through.

However, for membranes obtained after 10 and 20 minutes of electrospinning, the exponent n takes a value of 0.5 or very close to 0.5. It indicates that diffusion is the mechanism controlling the release of ibuprofen. Therefore, drug transport initially occurs through the dissolution of the drug through the membrane, which is followed by diffusion through the same membrane and desorption to the other side of the membrane. Considering that the release of ibuprofen is controlled by diffusion, it is possible to apply the classical Higuchi equation (eq. 3), to determine the mass transport coefficient, and then the approach of Fick's second law

to determine the apparent diffusivity of ibuprofen through the PLA membranes obtained after 10 and 20 minutes of electrospinning.

Table 11: Drug release parameters for PLA membranes obtained after 10 and 20 minutes of electrospinning.

Electrospinning time (min)	*Ibuprofen amount (mg)*	K_H	*Diffusivity (cm^2/s)*
10	5	0.033	1.8395E-08
10	10	0.030	2.2564E-08
10	15	0.029	3.3436E-08
20	5	0.028	2.1899E-08
20	10	0.026	2.6895E-08
20	15	0.023	2.8468E-08

The data presented in **Table 11** shows that the mass transport coefficient, K_H, (equation (4)) for the release of ibuprofen through electrospinning membranes, decreased when membrane thickness is increased (from 10 to 20 min. electrospinning). This result is due to the reinforcement of fibers, which become denser and not easily penetrable. This fiber reinforcement reduces the empty spaces available for ibuprofen particle mobility, which restrains its transference to the external medium. Increasing the drug concentration further decreases the available empty spaces for mass transference, which consequently decreases the mass transport coefficient.

Table 11 also shows the diffusivity *(D)* values, which appear to increase for the 10 min. electrospinning membrane when the initial drug concentration is increased.

Increasing the electrospinning time from 10 to 20 min. produces even denser membranes that are full of fibers with a compact internal structure and less empty spaces for particle mobility and transport. Therefore, increasing the ibuprofen concentration fills even more of the empty spaces in the membrane, which decreases the possibility of internal transport and consequently decreases the mass transport coefficient and restrains the drug delivery, as shown in **Table 11**.

Unlike the 10 min. electrospinning membrane, the diffusivity of ibuprofen through the 20 min. electrospinning membrane is practically constant with increasing drug concentration, as the variation in the diffusivity values is insignificant. This is due to the uniformity of membrane thickness. The minor variation in diffusivity shown for the 20 min. electrospinning membrane could be attributed to theoretical fitting uncertainty. Here, it is possible to maintain the percentage of drug release disregarding the amount of drug in the reservoir. The average value of diffusivity shown in **Table 11** is 2.5 E-08 cm^2/s, in accordance with the common range of drug diffusivities in various membranes [84,85].

5. References

1. Wachter, R., WEUTHEN, M., PANZER , C. & PAFF, E. 2005. Liposomes are used as textile finishes which not only improve elasticity and hand but can also be transferred to skin contact. Patent nº EP1510619-A2. DE10339358-A1. US2005058700-A.

2. GUARDUCCI, M. 2006. Product having particular functional properties for the skin and process for the preparation thereof. Patent no. WO/2006/106546.

3. Hipler, U.C. and Elsner, P. (2006). Biofunctional textiles and the skin. In: Burg G (eds) Curr. Probl. Dermatol. 1st ed. vol.33. asel: Karger.

4. 4.SCHAEFER, H., REDELMEIER, T.E. 1996. In: Skin barrier: Principles of percutaneous absorption, Karger. Basel and New York.

5. OCDE, Skin Absorption: In Vitro Method, Guideline 428, Guidelines for the Testing of Chemicals, Paris, France, (2004).

6. Kalia YN, Guy RH. Modeling transdermal drug release. Advanced Drug Delivery Reviews, 2001; 48:159-172.

7. Baker RW, Lonsdale HK. 1974. Controlled release: mechanisms and rates, Controlled Release of Biologically Active Agents, Plenum Press, New York 15–72.

8. Grassi M, Grassi G, Lapasin R, Colombo I. 2007. Understanding drug release and absorption mechanisms, Taylor and Francis Group, Chapter 9, 583-584.

9. Harland RS, Peppas NA, On the accurate experimental determination of drug diffusion coefficients in polymers, S.T.P. Pharm Sci, 1993; 3:357.

10. Tojo K, Sun Y, Ghannam MM, Chien YW. Characterization of a membrane permeation system for controlled delivery studies, AIChE J, 1985; 31:741-746.

11. Laghoueg N, Paulet J, Taverdet JL, Vergnaud JM. Oral polymer–drug devices with a core and an erodible shell for constant drug delivery, Int J Pharm, 1989; 50:133-139.

12. Lavasanifar A, Ghalandari R, Ataei Z, Zolfaghari ME, Mortazavi SA. Microencapsulation of theophylline using ethylcellulose: in vitro drug release and kinetic modelling, J Microencapsul, 1997; 14:91-100.

13. Lorenzo-Lamosa ML, Remuñan-López C, Vila-Jato JL, Alonso HJ. Design of microencapsulated chitosan microspheres for colonic drug delivery, J Contr Rel, 1998; 52:109-118.

14. Ouriemchi EM, Vergnaud JM. Processes of drug transfer with three different polymeric systems with transdermal drug delivery, Comput Theor Polym Sci, 2000; 10:391-401.

15. Carreras N, Acuña V, Martí M, Lis MJ. Drug release system of ibuprofen in PCL-microspheres. Colloid Polym Sci 291:157–165. 2013

16. 16.Yamashita F, Hashida M, Mechanistic and empirical modeling of skin permeation of drugs, Advanced Drug Delivery Reviews, 2003; 55:1185-1199.

17. 17.Grassi M. 2007. Membranes in drug delivery, in Handbook of membrane separations: chemical, pharmaceutical, and biotechnological applications, Sastre, A.M., Pabby, A.K., Rizvi, S.S.H., Eds., Marcell Dekker.

18. Flynn GL, Yalkowsky SH, Roseman TJ. Mass transport phenomena and models: theoretical concepts, J Pharm Sci, 1974; 63:479.

19. Grassi M, Grassi G. Mathematical modelling and controlled drug delivery: matrix systems, Curr Drug Deliv, 2005; 2:97.

20. Inoue SK, Guenther RB, Hoag SW, Algorithm to determine diffusion and mass transfer coefficients, in Proceedings of the Conference on Advances in Controlled Delivery, 145 (1996).

21. Grassi M, Grassi G, Lapasin R, Colombo I. 2007. Understanding drug release and absorption mechanisms, Taylor and Francis Group, Chapter 9, 583-584.

22. Colombo I, Grassi M, Lapasin R, Pricl S. Determination of the drug diffusion coefficient in swollen hydrogel polymeric matrices by means of the inverse sectioning method, J. Contr. Rel. 1997; 47:305-314.

23. Guy RH, Hadgraft J. A theoretical description relating skin penetration to the thickness of the applied medicament. Int J Pharm, 1980; 6:321–332.

24. Pharmacy - Encyclopedia Of Controlled Drug Delivery, V 1&2, (1999) 495-497.

25. Mathiowitz E. Pharmacy - Encyclopedia of Controlled Drug Delivery. vol 1&2. Wiley, Providence, 1999.

26. Abdekhodaie MJ, Cheng Y–L. Diffusional release of a dispersed solute from planar and spherical matrices into finite external volume. Journal of Controlled Release 1997; 43: 175-182.

27. Siepmann J, Lecomte F, Bodmeier R. Diffusion- controlled drug delivery systems: Calculation of the required composition to achieve desired release profiles. Journal of Controlled Release 1999; 60: 379-389.

28. Siepmann J, Kranz H, Bodmeier R, Peppas NA. HPMC – Matrices for Controlled Drug Delivery: A new Model Combining Diffusion, Swelling, and Dissolution Mechanisms and Predicting the Release Kinetics. Pharmaceutical Research 1999; 16: 1748-1756.

29. Siepmann J, Peppas NA. Modelling of drug release from delivery systems based on hydroxypropyl methylcellulose (HPMC), Advanced Drug Delivery Reviews 2001; 48: 139-157.

30. Kumari K, Kundu PP. Studies on in vitro release of CPM from semi-interpenetrating polymer network (IPN) composed of chitosan and glutamic acid. Bulletin of Materials Science 2008.; 31: 159-167.

31. Brazel, C.S., Peppas, N.A., 2000. Modeling of drug release from swellable polymers. European Journal of pharmaceutics and biopharmaceutics, 49, 47-58.

32. Peppas NA, Keys KB, Torres – Lugo M, Lowman AM. Poly (ethylene glycol) – containing hydrogels in drug delivery. Journal of Controlled Release 1999; 62: 81-87.

33. Rubio L, Alonso C, Coderch L, Parra JL, Martí M, Cebrián J, Navarro JA, Lis M, Valldeperas J, Skin delivery of caffeine contained in biofunctional textiles, Text Res J, 2010; 80:1214-1221.

34. Marti M, Martínez V, Carreras N, Alonso C, Lis M, Parra JL, Coderch L. Textiles with gallic acid microspheres: in vitro release characteristics. J.of Microencapsulation, 2014; Doi:10.3109/02652048.2014.885605.

35. Shaoabing Z, Xianmo D, Hua Y. Biodegradable poly(ε-caprolactone) - poly (ethyleneglycol) block copolymers: characterization and their use as drug carriers for a controlled delivery system. Biomaterials, 2003; 24:3563-3570.

36. 36.HUTMACHER, D. W. 2000. Scaffold in tissue engineering bone and cartilage. Biomaterials, 21, 2529-2543.

37. W.J. Yen, B.S. Way, L.W. Chang, P.D. Duh, Antioxidant properties of roasted coffee residues, J. Agric. Food Chem., 53, (2005) 2658-2663.

38. Parra J.L., Pons L. 1995, in: Cons. Gen. Col. Of. Farm. (Ed), Ciencia Cosmética, Madrid pp.512.

39. Conney A.H., Lu Y.P., Lou Y.R., Huang M.T. 2002. Inhibitory effects of tea and caffeine on UV-induced carcinogenesis: Relationship to enhanced apoptosis and decreased tissue fat, Eur. J. Cancer Prev. 11: S28-S36.

40. Thiele, J.J., Dreher, F., Packer, L., 2000. Antioxidant defense systems in skin, in: P. Elsner, H. Maibach (eds) Drugs

vs. Cosmetics: Cosmeceutical?. Dekker, New York, pp. 145-187.

41. Ting WW, Vest CD, Sontheimer R. Practical and experimental consideration consideration of sun protection in dermatology. Int J Dermatol 2003; 42: 505-513.

42. Lian T, Ho RJY. Trends and developments in liposome drug delivery systems. J Pharm Sci, 2001; 90: 667-680.

43. 43.Teschke O, de Souza EF. Liposome structure imaging by atomic force microscopy: verification of improved liposome stability during absorption of multiple aggregated vesicles. Langmuir, 2002; 18: 6513-6520.

44. Betz G, Aeppli A, Menshutina N, Leuenberger H. In vivo comparison of various liposome formulations for cosmetic application. Int J Pharm, 2005; 296: 44-54.

45. Aggarwal A, Dayal A, Kumar N. Microencapsulation processes and application in textile processing. Colourage, 1998; 45(8):15-24.

46. Martí M, de la Maza A, Parra JL, Coderch L. Dyeing Wool al Low Temperatures: New Method Using Liposomes. Text Res J, 2001; 71(8): 678-682.

47. Montazer M, Validi M, Toliyat T. Influence of temperature on stability of multilamellar liposomes in wool dyeing. J Liposome Res, 2008 ; 16(1): 81-89.

48. Martí M, de la Maza, A. Parra J.L. and Coderch, L. Role of Liposomes in Textile Dyeing. Liposomes, Lipid Bilayers and Model Membranes. From basic Research to Application. Pabst, G., Kucerka, N., Nieh, M-P., Katsaras, J. eds. CRC Press 2014

49. Martí M, de la Maza A, Parra JL and Coderch L, LIPOSOME AS DISPERSING AGENT INTO DISPERSE DYE FORMULATION Textile Research Journal 81(4): 379-387; 2011

50. Ramirez R, Martí M, Manich AM, Parra JL, Coderch L. Ceramides Extracted from Wool: Pilot Plant Solvent. Textile Res J, 2008; 78: 73-80.

51. Coderch L, Fonollosa J, Martí M, Garde F, de la Maza A, Parra JL. Extraction and Análisis of Ceramides from Internal Wool Lipids. J Am Oil Chem Soc, 2002; 79: 1215-1220.

52. Coderch L, Fonollosa J, de Pera M, de la Maza A, Parra JL, Martí M. Compositions of internal lipid extract of wool and use thereof in the preparation of products for skin care and treatment. 2001: Patent nº WO/2001/004244.

53. Carreras, N., Acuña, V., Martí, M., Lis, M.J., 2013. Drug release system of ibuprofen in PCL-microspheres. Colloid Poly Sci., 291, 157-165.

54. Ramírez R, Martí M, Barba C, Méndez S, Parra JL, Coderch L. Skin Efficacy of liposomes composed of internal wool lipids rich in ceramides. J Cosmet Sci, 2010; 61: 235-245.

55. Rougier A, Dupuis D, Lotte C, Rouguet R, Shaefer H. In vivo correlation between stratum corneum reservoir function and percutaneous absorption. J Invest Dermatol, 1983; 81: 275-278.

56. Rougier A, Dupuis D, Lotte C, Roguet R, Wester RC, Maibach HI. Regional variation in percutaneous absorption in man: measurement by the stripping method. Arch Dermatol Res, 1986; 278: 465–469.

57. Pinkus H. Examination of the epidermis by the strip method of removing horny layers. I. Observation on thickness of the horny layer, and on mitotic activity after stripping. J Invest Dermatol, 1951; 16: 383–386.

58. Ramón E, Alonso C, Coderch L, De la Maza A, López O, Parra JL, Notario J. Liposomes as Alternative Vesicles for Sun Filter Formulations. Drug Delivery, 2005; 12: 83-88.

59. Martí M, Rodrígueza R, Carreras N, Lis M, Valldeperas J, Coderch L, Parraa L. Monitoring of the icrocapsule/ liposome application on textile fabrics, J. of the Textile Institute 103: 19-23, 2012

60. Carrión, F.J. (1986). Characterization of the electric double layer in textile fibers and its influence on the absorption of surfactants. Bol. Intexter., 90, 25-47.

61. Cutler, W.G. and Davis, R.C. (1972). Ed. Detregency Theory and Test Methods. Part I, Vol 5, Surfactant Sciences Series. Ed. Marcel Dekker Inc. New York.

62. López, O., de la Maza, A., Coderch, L., López-Iglesias, C., Wehrli, E. and Parra, J.L. (1998). Direct formation of mixed micelles in the solubilization of phospholipid liposomes by Triton X-100. FEBS Letters, 426, 314-318.

63. López, O., de la Maza, A., Barbosa, L., García Antón, J.M., Cebrián, J., Albiñana, N. (2009). Cosmetic of dermopharmaceutical composition of mixed Micelles. Pat. WO/2009/106338.

64. López, O., Cócera, M., López-Iglesias, C., Walter, P., Coderch, L., Parra, J.L. and de la Maza, A. (2002). Reconstitution of liposomes inside the intercellular lipid domain of the stratum corneum. Langmuir, 18, 7002-7008.

65. Baptista, A.L.F., Countinho, P.J.G., Real Oliveira, M.E.C.D. and Rocha Gomes, J.I.N. (2004). Lipid interaction with textile fibers in dyeing conditions. Progr. Colloid Polym Sci., 123, 88-93.

66. Y.C. Kim, J.H. Park, M.R. Prausnitz, Microneedles for drug and vaccine delivery, Adv Drug Deliv Rev. 64 (2012) 1547–1568.

67. J.H. Park, G.Saravanakumar, K. Kim, I.C. Kwon, Targeted delivery of low molecular drugs using chitosan and its derivatives, Adv Drug Deliv Rev. 62 (2010) 28–41.

68. Y.Zhang, H.F. Chan, K.W. Leong, Advanced materials and processing for drug delivery: The past and the future, Adv Drug Deliv Rev. 65 (2013) 104–120.

69. A.M. Wokovicha, S. Prodduturia, W.H. Douba, A.S. Hussainb, L. F. Buhse, Transdermal drug delivery system (TDDS) adhesion as a critical safety, efficacy and quality attribute, Eur J Pharm Biopharm. 64 (2006) 1–8.

70. J. Siepmann, N.A. Peppas, Higuchi equation: Derivation, applications, use and misuse, Int J Pharm. 418 (2011) 6–12.

71. A. Davidsona, B.A. Qallafb, D.B. Dasc, Transdermal drug delivery by coated microneedles: Geometry effects on effective skin thickness and drug permeability,

Chem Eng Res Des. 86 (2008) 1196–1206.

72. R. Langer, L.G. Cima, J.A. Tamada, E. Wintermantel, Future directions in Biomaterials, Biomaterials. 11 (1990) 738-745.

73. G. Ponchel, J.M. Irache, C. Durrer, D. Duchene, Proc. Int. Symp. Controlled Release Bioact Mater. 21 (1994) 31-32.

74. A.T. Raiche, D.A. Puleo, Modulated release of bioactive protein from multilayered blended PLGA coatings, Int J Pharm. 311 (2006) 40–49.

75. B. Guptaa, N. Revagadea, J. Hilborn, Poly(lactic acid) fiber: An overview, Prog Polym. Sci. 32 (2007) 455–482.

76. R. Auras, L.-T. Lim, S.E.M. Selke, H. Tsuji, Poly(Lactic Acid): Synthesis, Structures, Properties, Processing, and Applications, John Wiley & Sons, Inc, New York, 2010.

77. A.C. Vieira, J.C. Vieira, R.M. Guedes, A.T. Marques, Experimental degradation characterization of PLA-PCL, PGA-PCL, PDO and PGA fibers, 17th International Committee on Composite Materials, 2009.

78. R. W. Field, K. F. Yunos, Z. Cui. Separation of proteins using sandwich membranes, Desalination. 246 (2009) 224–232.

79. H.L.G.M. Tiemessen, H.E. Bodd, H.E. Junginger. A silicone membrane sandwich method to measure drug transport through isolated human stratum corneum having a fixed water contente. Int J Pharm. 56 (1989) 87-94.

80. D.H. Reneker, A.L. Yarin, Electrospinning jets and polymer nanofibers, Polymer 49 (2008) 2387-2425.

81. J. Zeng, X. Xu, X. Chen, Q. Liang, X. Bian, L. Yang, X. Jing, Biodegradable electrospun fibers for drug delivery, J Control Release. 92 (2003) 227–231.

82. D.F. Stamatialis, B.J. Papenburg, M. Gironés, S. Saiful, S.N.M. Bettahalli, S . Schmitmeier, M. Wessling, Medical applications of membrane: Drug delivery, artificial organs ans tissue engineering, J Membrane Science. 308 (2008) 1-34.

83. A. P. S. Immich, M.J. Lis Arias, N. Carreras, R. L. Boemo, J. A. Tornero. Drug delivery systems using sandwich configurations of electrospun poly(lactic acid) nanofiber membranes and ibuprofen. Materials Science and Engineering C 33 (2013) 4002–4008.

84. J. Siepmann, N.A. Peppas, Modeling of drug release from delivery systems based on hydroxylpropyl methylcellulose (HPMC), Adv Drug Deliv Rev. 48 (2001) 139-157.

85. Y. Chen, Y. Zhang , X. Feng, An improved approach for determining permeability and diffusivity relevant to controlled release, Chem Eng Sci. 65 (2010) 5921–5928.